Sustainable Food Technology

ROYAL SOCIETY OF CHEMISTRY

PAPER

View Article Online
View Journal | View Issue

Open Access Article. Published on 21 April 2023. Downloaded on 1/12/2026 11:32:11 PM.
This article is licensed under a Creative Commons Attribution-NonCommercial 3.0 Unported Licence.

Check for updates

Cite this: *Sustainable Food Technol.*, 2023, **1**, 437

Sustainable processing of Greek yogurt acid-whey waste to develop folic acid encapsulated millet powders

Sargun Malik,[a] Mohamed B. Bayati,[b] Chung-Ho Lin[bc] and Kiruba Krishnaswamy *[ad]

Received 21st January 2023
Accepted 26th March 2023

DOI: 10.1039/d3fb00009e

rsc.li/susfoodtech

Folic acid is an essential nutrient that is required to prevent anemia in women and neural tube defects in infants. Hence, it is important to develop food products that can act as a source of folic acid and are easily accessible. For product development, two encapsulation methods were used: spray drying and extrusion. The encapsulated powder was formed using the matrix of acid whey, kodo, and proso millet. The extrusion method used a folic acid-alginate solution that was dispensed in cross-linking solutions containing acid whey and millets. The objective of the paper was to analyze the developed products for shelf stability and commercial viability. Adding millets to acid whey led to a high yield and the obtained powder was free-flowing. The encapsulated capsules were stable in different pH conditions. The *in vitro* digestibility model indicated that both powder mix and alginate capsules were efficient sources of folic acid.

1 Introduction

According to the World Health Organization (WHO), 29.9% of women of reproductive age (15–49 years) suffer from anemia wherein 36.5% of pregnant women are anemic globally.[1] Folate-deficiency acid anemia occurs when the folic acid in the blood is not enough further causing megaloblastic anemia wherein the red blood cells are fewer and larger than normal complicating the pregnancy.[2] In addition, folic acid deficiency can also cause neural tube defects as folic acid helps in the formation of the neural tube. Hence, folic acid is important to prevent major defects such as anencephaly and spina bifida. Consequently, the Centers for Disease Control and Prevention has recommended that all women of reproductive age should have at least 400 mg of Dietary Folate Equivalent (DFE) of folic acid and pregnant women should consume 600 mg of DFE daily to prevent neural tube defects in babies.[3]

Folic acid (Vitamin B9) is one of the most essential nutrients that naturally occur as folate. The primary function of folate is that it acts as a coenzyme in the single-carbon transfer that further leads to the synthesis of DNA and RNA. It also helps in the metabolism of amino acids. The dietary source of folate includes raw green leafy vegetables, seafood, nuts, broccoli, brussels sprouts, kale, *etc.*[4] Folic acid is the fully oxidized monoglutamate form of folate composed of pteridine, *p*-aminobenzoic acid (PABA), and glutamic acid. The folates present in food products are very sensitive to the environment, for example, high-temperature conditions, UV light, metal ions, and extreme pH changes. If the food product is stored for a long time, there is oxidation, and it gets converted to its derivative compounds. Processing can also reduce the vitamin content by 50–80%, especially in thermal processing.[5]

Encapsulation of bioactive ingredients helps in increasing the shelf life of a product, protecting it from any adverse environmental condition such as extreme temperature, light, oxygen, pH, moisture, *etc.* It involves entrapping or coating the active agent into a wall material or carrier agent. These carrier agents can be made from different polysaccharides, proteins, and lipids.[6] There are various methods through which encapsulation of functional components can be done such as spray drying, extrusion methods, coacervation, spray cooling, *etc.*[7] Spray drying is a common and extensively used bottom-down technique for microencapsulation in which a liquid feed is atomized into a drying chamber wherein it undergoes rapid evaporation, as it encounters a drying medium such as hot air.[8] The liquid feed containing the wall material converts into a powder that encapsulates the functional ingredient.[9] Similarly, extrusion is a top-down technique wherein a solution containing an active agent and carrier agent such as alginate is passed through a nozzle to a gelling environment. Alginate is a polysaccharide that is derived from brown algae and can be used as a delivery system that preserves the bioactive component.[10] The ionic crosslinking is commonly used for this gelling process wherein wall material is combined with cross-linking agents such as divalent cations that combine with the guluronate blocks present in the alginate chain.[11]

In the domain of food security and nutrition, there is always an intersection of food loss and waste that needs to be addressed.[12]

[a]*Department of Food, Nutrition & Exercise Sciences, University of Missouri, Kiruba Krishnaswamy, 244, Agriculture Engineering Building, Columbia, MO, 65201, USA. E-mail: krishnaswamyk@umsystem.edu*

[b]*School of Natural Resources, University of Missouri, Columbia, MO, USA*

[c]*Center of Agroforestry, University of Missouri, Columbia, MO, USA*

[d]*Department of Biomedical, Biological and Chemical Engineering, University of Missouri, Columbia, MO, USA*

© 2023 The Author(s). Published by the Royal Society of Chemistry

Open Access Article. Published on 21 April 2023. Downloaded on 1/12/2026 11:32:11 PM.
This article is licensed under a Creative Commons Attribution-NonCommercial 3.0 Unported Licence.

The Greek yogurt processing generates a large quantity of acid whey that is dumped into the surroundings causing damage to the environment. This acid whey has been found to have different macro-micro nutrients and hence can be upcycled for the production of value-added products.[13] Likewise, millets are underutilized climate-resilient ancient grains.[14] The probiotic component from acid whey can be combined with the prebiotic component of millets to have a potential synbiotic food product.[15–17] The formed matrix can further be fortified with folic acid and spray dried for the production of a nutrition mix that can be utilized to fulfill the daily requirement of folic acid. Alternatively, the extrusion method can be used for the production of folic acid capsules wherein folic acid can be combined with sodium alginate and dropped into a millet-acid whey matrix that is rich in minerals and hence, a source of cations and anions for crosslinking.

Hence, the objective of the paper is to develop a folic acid-based food ingredient with the aid of acid whey and millets. The study aims to analyze the physicochemical characteristics of the constructed food ingredients and evaluate its shelf stability and consequently commercial viability.

2 Material & methods

2.1 Development of encapsulated product

2.1.1 Preparation of folic acid encapsulated powder. The sample matrix was prepared by mixing 50 g kodo and proso millet (Manna ethnic millets®, Chennai, India) powder and 250 mg folic acid in the 100 mL acid whey. The folic acid was purchased from Sigma Aldrich (Cas no. 59-30-3, St Louis, MO, USA). The millet powder used for the matrix was obtained by milling the kodo and proso millet grains respectively in a mixer grinder (Butterfly Rapid Mixer Grinder™, Butterfly Gandhimati Appliances®, Chennai, India) and sieving in a 20 cm diameter stainless steel sieve (Makerstep®, Cypress, CA, USA).

The utilized acid whey was separated from Greek yogurt prepared in the laboratory. Greek yogurt was prepared by first heating 1 L of pasteurized milk (Grade A, Vitamin D fortified whole milk, Central Dairy, Columbia, MO, USA) at 82 °C, cooling it to 43.3 °C before adding 10 g of starter culture (Chobani® Plain Greek Yogurt, Norwich, New York, USA). After the addition of culture, the product was kept in an incubator at 37 °C for 8 hours. Subsequently, the formed yogurt was filtered using a cheesecloth and acid whey was collected and stored at 4 °C.

For mixing all the three components (millet powder, folic acid, and acid whey), a homogenizer (IKA Eurostar 40, Wilmington, NC, USA) was used at 1000 rpm for 30 minutes. Two separate slurries were formulated wherein one contained kodo millet and the other contained proso millet. The slurries were then passed through a vacuum filtration process and the filtered liquid was collected and spray dried as shown in Fig. 1.

Spray drying operation was conducted on the vacuum-filtered permeates using a spray dryer (Mini Spray Dryer B-290, New Castle, DE, USA). The process was carried out at an inlet temperature of around 160 °C. The flowmeter for spraying air, feed flow rate, and aspiration rate was adjusted for obtaining maximum yield. Likewise, two types of powders were formed one containing kodo (KAWFP) and the other containing proso millet (PAWFP). After each run, the obtained powder was weighed and stored at 4 °C. The yield of the spray drying powder was calculated based on eqn (1).

$$\text{Yield } (\%) = \frac{\text{solid content in spray dried powder } (g)}{\text{solid content in the feed to be spray dried } (g)} \times 100 \quad (1)$$

2.1.2 Preparation of folic acid encapsulated alginate capsules. For the preparation of folic acid capsules, 100 mg of folic acid powder was added to 60 mL of 1% sodium alginate

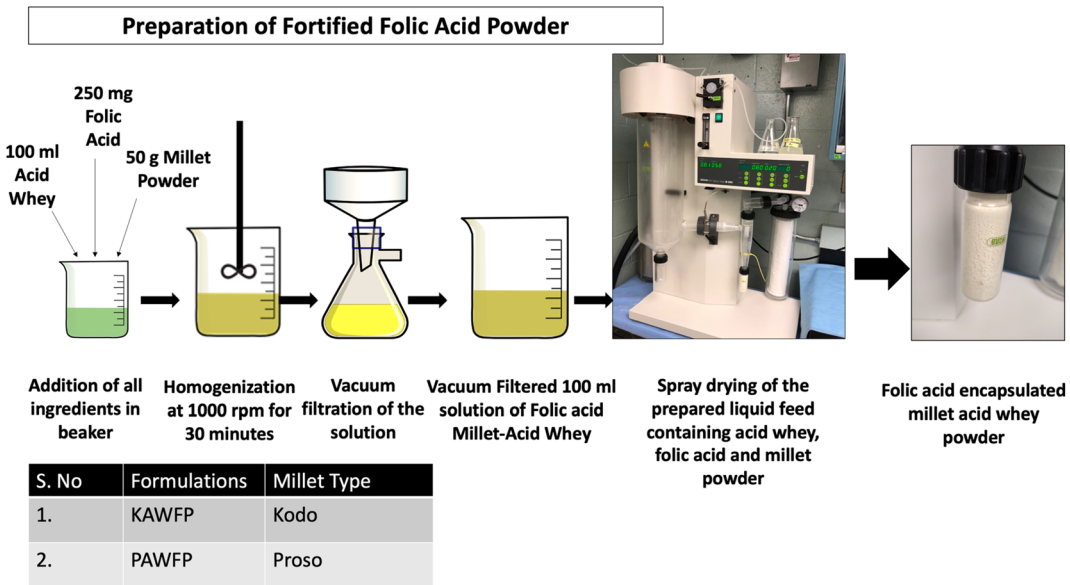

Fig. 1 Development of folic acid encapsulated powder using ingredients, acid whey from Greek yogurt processing, millets (kodo & proso), and folic acid.

 © 2023 The Author(s). Published by the Royal Society of Chemistry

Open Access Article. Published on 21 April 2023. Downloaded on 1/12/2026 11:32:11 PM.
This article is licensed under a Creative Commons Attribution-NonCommercial 3.0 Unported Licence.

solution and 40 mL of 0.1 M sodium bicarbonate solution. The solution was then mixed using a homogenizer at 750 rpm for 45 minutes. The solution was then drawn up in a 20 mL syringe and using a syringe pump was dropped in a 100 mL liquid of cross-linking solutions as shown in Fig. 2.

2.2 Folic acid content analysis in the developed products

2.2.1 Extraction of folic acid from the matrix. For folic acid extraction from the formed food product, 1 g of the sample was added to a 15 mL centrifuge tube. Ten milliliters of extraction solvent consisting of 1% glacial acetic acid in methanol was mixed with the sample. For the capsule samples, a mortar and pestle was used for grinding with the solvent. The solution was vortexed for 10 minutes until the powders were completely homogenized with the solvent. The mixture was sonicated for 30 minutes using a sonicator (Model no. 08895-21, Cold Palmer, Vernon hills, Illinois, USA) and centrifuged at 5000 rpm for 15 minutes. The supernatant of the sample was then passed through a 0.2 μm syringe filter (Whatman® Anotop®) with a diameter of 25 mm. The filtered extracts were then collected in 10 mL centrifuge tubes.

2.2.2 LC-MS/MS analysis. The concentration of folic acid was determined using a LC-MS/MS system (Waters Alliance 2695 HPLC system coupled with Waters Acquity TQ triple quadrupole mass spectrometer (MS/MS) Milford, MA, USA). The separation of folic acid was achieved using Phenomenex (Torrance, CA) Kinetex C18 (100 mm × 4.6 mm; 2.6 μm particle size) reverse-phase column. The mobile phase consisted of 100% acetonitrile (A) and 10 mM ammonium acetate and 0.1% formic acid in MilliQ water (B). The gradient conditions were 0–0.5 min, 2% A; 0.5–7 min, 2–80% A; 7.0–9.0 min, 80–98% A; 9.0–10.0 min, 2% A; at a flow rate of 0.5 mL min^{-1}. The ion source in the MS/MS system was electrospray ionization (ES) operated in the negative ion with a cone voltage of 50 V, the ionization source and desolvation temperature were programmed at 150 °C, and 750 °C respectively. The MS/MS system was operated in the multi-reaction monitoring (MRM) mode with the optimized collision energy of 22 eV wherein the molecular ion and product ion (m/z 440.35® 311.25) were determined from the spectra that were obtained from injection of 30 μL of the folic acid analytical standard of concentration 10 mg L^{-1}. For data analysis, Water Empower 3 software (Waters, CA, USA) was used. The signal-to-noise ratios of three and ten were employed to calculate LOD and LOQ, respectively.

The folic acid amount obtained from the analysis was used to calculate the encapsulation efficiency using eqn (2).

$$\text{Encapsulation efficiency (EE\%)} = \frac{\text{folic acid obtained in the final product (mg g}^{-1})}{\text{folic acid added in the matrix (mg g}^{-1})} \times 100 \quad (2)$$

2.3 Color analysis

The color analysis was conducted using a colorimeter (Konika Minolta® CR-410, Ramsey, New Jersey, USA) and based on to Commission Internationale d'Eclairage (CIE) LAB system. The samples were placed in a Petri dish and were gently spread. "L", "a" and "b" values were taken and using the obtained valued Hue (eqn (3)), chroma (eqn (4)), and whitening index (eqn (5)) were calculated.

$$\text{Hue angle} = \tan^{-1} b/a \quad (3)$$

$$\text{Chroma} = \sqrt{a^2 + b^2} \quad (4)$$

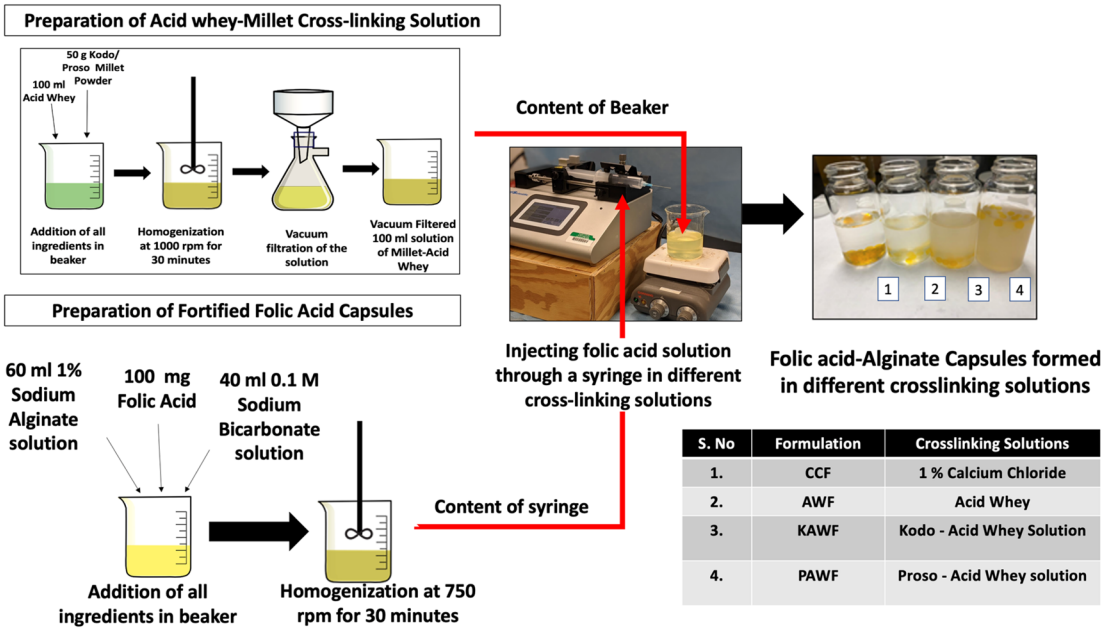

Fig. 2 Preparation of folic acid encapsulated capsules by the extrusion-based method using folic acid alginate gel and ionic crosslinking solutions. The ionic crosslinking solution includes calcium chloride,[1] acid whey,[2] kodo & acid whey solution[3] and proso & acid whey solution.[4]

Open Access Article. Published on 21 April 2023. Downloaded on 1/12/2026 11:32:11 PM.
This article is licensed under a Creative Commons Attribution-NonCommercial 3.0 Unported Licence.

$$\text{Whitening index} = 100 - \sqrt{(100 - L)^2 + \left((a)^2 + (b)^2\right)} \quad (5)$$

2.4 Moisture content and water activity

The moisture content was obtained using a moisture analyzer (Model HE53, Mettler Toledo, Columbus, OH, US). For measurement, 3 g of sample was weighed and poured over the aluminum dish where it was spread evenly. The water activity was measured using a water activity meter (Aqua lab model CX-2, Pullman, WA). For measurement, the water activity meter cups were filled with an appropriate amount of sample that permitted the required headspace. The readings were taken in triplicates.

2.5 Thermal analysis of samples

The thermal properties were analyzed using Differential Scanning Calorimeter (Thermal Analyzer instrument Q 20, New Castle, DE, USA). For measurement, 8 mg of sample was weighed and placed in an aluminum pan. Further, the pan was sealed and loaded into the instrument. The instrument was fixed at ramp mode wherein the heating rate was set at 10 °C min^{-1} and the temperature range was kept at 20 to 250 °C. The data was analyzed to obtain peak thermal degradation and glass transition temperature. The analysis was conducted in triplicates.

2.6 Particle size analysis

The mean diameter, mean polydispersity index (PDI), and zeta potential (ζ) were obtained using Dynamic Light Scattering (DLS) system (Delsa Nano Submicron Particle Size and Zeta Potential particle Analyzer, Beckman Coulter California, United States). The scattering angle of the system was adjusted at 15°. Water was used as a diluent for sample preparation. For the preparation of the sample, 1 g of powder was mixed with 10 mL of DI water to prepare a stock solution. The solution was further diluted by taking 200 μL of the stock solution and mixed 9.8 mL of DI water for DLS analysis.

For encapsulated capsules, open-source image processing FIJI software was utilized to calculate average diameter and sphericity. The sphericity was calculated by taking ratio of longest and shortest diameter.

2.7 Scanning electron microscopy

Scanning electron microscopy was used to analyze the morphology of the formed encapsulated powder and capsules. The analysis was conducted with the help of the Electron Microscopy Core Facility, University of Missouri-Columbia. The powder samples were sprinkled on the stub holders with the help of carbon tapes. To prevent clustering air was passed through the surface after the placing step. For the capsule samples, one to two capsules were placed. The samples were then sputtered with 25 nm Pt for the imaging in FEI Quanta 600F ESEM (Hillsboro, Oregon, United States). The images were taken under high vacuum conditions with the voltage of 5 kV, working distance adjusted to 8 mm, objective aperture of 30 μm, and 3.5 spot size. Energy-dispersive X-ray spectroscopy (EDS) analysis was conducted for the capsule samples to view morphology along with chemical composition.

2.8 Stability of folic acid capsules

2.8.1 pH. The pH was measured using a digital pH meter (Mettler Toledo™ Columbus, OH, USA) with a pH electrode (In Lab® Expert Pro-ISM). The samples were stored under different temperatures (5 °C and 25 °C) and light (light and dark) conditions and the pH was taken after 48 h. The results were then compared with the initial pH. Before taking the measurements, the pH meter was calibrated using a standardized buffer solution that was at pH 2.00, 4.00, 7.00, and 10.00. For each sample, three readings were taken.

2.8.2 Mechanical stability. The mechanical stability of alginate capsules was analyzed using a texture analyzer (TA-HDi, Texture Technologies Corp., Scarsdale, N.Y., USA). The texture analyzer was equipped with a 100 kg load cell with a cylindrical probe TA-93 of diameter 4 cm. The strain percentage was set at 60% and the pre-test, test, and post-test speeds were fixed at 0.5 mm s^{-1}. The data analysis was conducted with the help of software exponent connect. The maximum force needed for compression was obtained as a hardness value that further indicates the capsule's resistance to the compression of the probe.[18]

2.9 Functional properties of spray dried powder

2.9.1 Particle, bulk, tap density & porosity. The particle density was measured using a pycnometer (Quantachrome Ultra pycnometer 1000, Anton Paar, Boynton Beach, FL, USA). For the analysis, 1 g of powder was weighed and poured into the cell. The analysis was conducted under vacuum conditions. The tap density was measured by mechanically tapping the 10 mL graduated cylinder containing 1 g of sample. The tapping was done 1250 times using an electronic shaker (IKA-VIBRAX-VXR, Janke & Kunkel, Markham, ON, Canada). For bulk density measurements, about 1 g of the powder sample was gently poured into a 10 mL glass graduated cylinder. The volume on the graduated cylinder was noted. The calculations were done using eqn (6).[19] Using the values obtained from bulk density and true density, porosity was calculated based on eqn (8). The flowability of the powder was estimated using Carr's Index (eqn (9)) and Hausner's ratio (eqn (10)).

$$\text{Bulk density} \quad (\text{g mL}^{-1}) = \frac{\text{mass of the powdered sample (g)}}{\text{volume of powdered sample in the graduated cylinder(mL)}} \quad (6)$$

 © 2023 The Author(s). Published by the Royal Society of Chemistry

Open Access Article. Published on 21 April 2023. Downloaded on 1/12/2026 11:32:11 PM.
This article is licensed under a Creative Commons Attribution-NonCommercial 3.0 Unported Licence.

$$\text{Tap density } (\text{g mL}^{-1}) = \frac{\text{mass of the powdered sample (g)}}{\text{volume of powdered sample after tapping grad. cylinder (mL)}} \quad (7)$$

$$\text{Porosity} = 1 - \frac{\text{bulk density } (\text{g mL}^{-1})}{\text{absolute density } (\text{g mL}^{-1})} \quad (8)$$

$$\text{Hausner ratio} = \frac{\text{tap density } (\text{g mL}^{-1})}{\text{bulk density } (\text{g mL}^{-1})} \quad (9)$$

$$\text{Carr index (CI\%)} = \frac{\text{tap density}(\text{g mL}^{-1}) - \text{bulk density}(\text{g mL}^{-1})}{\text{tap density}(\text{g mL}^{-1})} \times 100 \quad (10)$$

2.9.2 Angle of repose. For calculation of the angle of repose, 5 g of powdered sample was gently passed through a plastic funnel with an outlet diameter of 1 cm. The height and base diameters of the obtained heap was noted for the calculation of the tan θ value. The calculations were done using eqn (11).[20]

$$\text{Tan } \theta = \frac{2 \times \text{height (cm)}}{\text{base diameter (cm)}} \quad (11)$$

2.9.3 Hygroscopicity. The hygroscopicity was observed by weighing 1 g of spray dried powder on a 5 cm diameter Petri dish and placing it in a desiccator wherein the humidity was set at 75% RH. The humidity was set using sodium chloride wherein 200 g of salt was mixed with 100 mL of DI water. The stored powder was weighed again after 24 hours, and the absorbed water amount was found. The result was then calculated according to eqn (12), as the amount of water absorbed (g) per g of dry solids.[21]

$$\text{Hygroscopicity (\%)} = \frac{\text{final weight of stored powder (g)} - \text{initial weight of stored powder (g)}}{\text{initial weight of stored powder (g)}} \times 100 \quad (12)$$

$$\text{Dispersibility\%} = \frac{[10 + \text{weight of powder}) \times \text{\% total solid in filtered permeate}}{\text{weight of powder } [100 - \text{moisture content of powder \%}][100 - \text{moisture content of powder \%}]/100} \quad (15)$$

2.9.4 Water solubility. For water solubility, 1 g of the sample was weighed and mixed with 15 mL DI water in a 50 mL centrifuge tube. The solution was vortexed for one minute. The tube was then shaken in a constant temperature water bath (Yamato™, Model number BT-25, Tokyo, Japan) for 30 minutes at 37 °C. Centrifugation was done at 3018.6×g for 5 minutes at 25 °C and the supernatant was poured into an aluminum dish and weighed. The solution was then dried in an oven (Unity™ Lab Services EWINC15, Thermo Fisher Scientific, Waltham, MA, USA) at 105 °C until complete drying and the weight of the dried powder was noted.[22] The calculation was conducted based on eqn (13).

$$\text{Water solubility\%} = \frac{\text{weight of dried supernatant (g)}}{\text{weight of dry powdered sample (g)}} \times 100 \quad (13)$$

2.9.5 Dispersibility. For obtaining dispersibility percentage, 1 g of the sample powder was weighed and mixed with 10 mL of DI water in a 50 mL beaker. The solution was then mixed well using a spatula and was through a 212 μm sieve (#4041, Hogentogler, CO, MD, USA). The permeate was collected and weighed in an aluminum dish. The total solid content of permeate and moisture content of powder were also obtained. For total solid content, the filtered solution was dried in an oven (Unity™ Lab Services EWINC15, Thermo Fisher Scientific, Waltham, MA, USA) at 105 °C for 30 min. After complete drying, the weight of aluminum dish was taken, and the solid matter was estimated based on eqn (11). The moisture content values were obtained using moisture analyzer (Model number HE53, Mettler Toledo, Columbus, OH, USA) and calculations were done based on eqn (14) and (15).

$$\text{Total solid\%} = \frac{\text{weight of dry matter in filtered permeate (g)}}{\text{weight of liquid filtered permeate (g)}} \times 100 \quad (14)$$

2.9.6 Rheological properties measurement. Rheological properties of the reconstituted samples were determined with rheometer (Anton Paar Rheo MCR 302 modular compact, Vernon Hills, Illinois, USA). The reconstitution of the samples was done by mixing 1 g of the powder with 10 mL of DI water. The instrument was equipped with a cone (25 mm diameter, 1° angle) and plate geometry. Flow behavior was analyzed using the Power Law model. Each sample was measured in triplicate.

Open Access Article. Published on 21 April 2023. Downloaded on 1/12/2026 11:32:11 PM.
This article is licensed under a Creative Commons Attribution-NonCommercial 3.0 Unported Licence.

2.9.7 Refractive index. The reconstituted sample was analyzed for refractive index (% Brix). For measurement, 1 g of the powder was mixed with 10 mL of DI water. A digital refractometer (WM-7 ATAGO™, Bellevue, WA, USA) was used for the analysis wherein one to two drops of the sample were poured on the prism of the device and the Brix value was noted. The measurement was conducted in triplicate.

2.10 *In vitro* digestibility

The *in vitro* digestibility analysis was conducted based on the protocol by Minekus *et al.*[23] For the analysis of salivary phase digestibility, 5 mL of reconstituted spray dried sample (PAWFP) and 5 g capsule (PAWF) sample were taken respectively and mixed with 3.5 mL of electrolyte solution. The electrolyte solution was prepared by mixing 15.1 mL of 0.5 M potassium chloride, 3.7 mL of 0.5 M potassium phosphate, 6.8 mL of 1 M sodium bicarbonate, and 0.5 mL of 0.15 M magnesium chloride, 0.06 mL of 0.5 M ammonium carbonate and 373.35 mL of DI water. Mincing of the food was done using a mortar pestle until paste-like consistency was achieved. To the paste, 0.5 mL of salivary α-amylase of activity 75 U mL^{-1} was added which was followed by the addition of 25 μL of 0.075 mM calcium chloride. The whole solution was maintained at pH 7 and was kept in the incubator at 37 °C for 2 minutes.

For the gastric phase, the 10 mL of oral bolus was mixed with 7.5 mL of gastric phase electrolyte solution. The electrolyte solution was prepared by mixing 6.9 mL of 0.5 M potassium chloride, 0.9 mL of 0.5 M potassium phosphate, 12.5 mL of 1 M sodium bicarbonate, 11.8 mL of 2 M sodium chloride, 0.4 mL of 0.15 M magnesium chloride, 0.5 mL of 0.5 M ammonium carbonate and 371 mL of DI water. To the gastric solution, 1.6 mL of porcine pepsin of activity 2000 U mL^{-1} was added, followed by 5 μL of 0.075 M of calcium chloride. The solution was maintained at pH 3 by the addition of 1 M hydrochloric acid and was incubated for 2 hours at 37 °C.

For the intestinal phase, the 20 mL gastric chyme was mixed with 11 mL of intestinal electrolyte solution. The electrolyte solution was prepared by mixing 6.8 mL of 0.5 M potassium chloride, 0.8 mL of 0.5 M potassium phosphate, 42.5 mL of 1 M sodium bicarbonate, 9.6 mL of 2 M sodium chloride, 1.1 mL of 0.15 M magnesium chloride and 339.2 mL of DI water. To the intestinal solution 5 mL of pancreatin from the porcine pancreas of activity 100 U mL^{-1} and lipase of activity 2000 U mL^{-1} was added, followed by the addition of 2.5 mL bile salts and 1.31 mL of DI water. The intestinal solution was maintained at pH 7 by addition of 1 M sodium hydroxide and incubated for 2 hours at 37 °C.

From each phase after incubation, 1 mL of solution was drawn for folic acid extraction and ran in the LC-MS/MS system.

2.11 Statistical analysis

The statistical analysis was conducted using JMP software (Cary, NC, USA). One-way ANOVA was used for confirming the difference among samples. For the post-hoc test, Tukey's honest significant difference test was used as it helps in explaining the pairwise difference among the samples. The significance of the results was considered at an alpha value of 0.05.

3 Results & discussion

3.1 Percentage yield & encapsulation efficiency

Spray drying is one of the most extensively used techniques for biologically sensitive material with only a slight loss in activity.[24] Even with a high inlet temperature of 160 °C, there is not much deterioration because of a small residence time of the droplet in the drying chamber of approximately 12 to 30 seconds and subsequent evaporative cooling effect.[25] The product yield of 71.49 ± 1.35% was obtained for KAWFP and 76.23 ± 2.65% for PAWFP. A high percentage indicates that the powder was not sticky and was able to be recovered from the collection chamber.

Usually, acid whey due to its low pH range (3.6–4.5) is challenging to process. This difficulty is attributed to the behavior of lactose with the present whey proteins, organic acids, and minerals. The crystallization of lactose also gets affected by the pH which further affects the processing performance. Millets being of alkaline nature help in neutralizing the acid whey which further helps in processing.[14,26] Folic acid has a low aqueous solubility of about 0.01 mg mL^{-1} below pH 5 and when it is dispersed in water, the pH is in the range of 4 to 4.8. However, it has good stability in the buffer solutions having a pH of 5.39 to 10.40.[27] The pH of the prepared feed containing folic acid, millet, and acid whey was 4.78 and 5.09 for kodo and proso millet species respectively. Since the pH was lower than the stability requirement, the liquid feed had a lot of undissolved folic acid settled at the bottom of the flask forming a cake. A substantial amount of folic acid was lost during the vacuum filtration step. Consequently, the encapsulation efficiency % of folic acid when calculated based on the folic acid present in the powder and added in the matrix, varied from 1.65–1.73%. Fig. 3 illustrates the final powder product formed by the spray dryer. The amount of folic acid obtained in the final encapsulated powders, KAWFP, and PAWFP were found to be similar as shown in Fig. 4 ($p > 0.05$).

The commercial vitamin mixes are available in form of sachets that contain around 6.5 g (0.22–0.23 onz) of powder. According to the said quantity, if a similar amount of powder was to be used, the powder samples would have been able to contain 850.2 μg and 806 μg of folic acid in the samples PAWFP and KAWFP respectively. These values are equivalent to 510.12 and 483 Dietary Folate Equivalent (DFE) μg respectively exceeding the daily required value of folic acid for adult males and females *i.e.*, 400 μg DFE. This additional amount of folic acid (80–110 μg DFE) was considered permissible, considering the loss of folic acid during storage of the powder.

The entrapment or encapsulation efficiency is dependent on the film-forming capacity and plastic behavior of the biopolymer that is mixed in the matrix. The commercially available encapsulating agents have limitations in terms of cost, availability, and potential damage to human health. For example, maltodextrin is a refined carbohydrate that can have a strong effect on blood glucose, insulin, and lipid level in the

 © 2023 The Author(s). Published by the Royal Society of Chemistry

Open Access Article. Published on 21 April 2023. Downloaded on 1/12/2026 11:32:11 PM.
This article is licensed under a Creative Commons Attribution-NonCommercial 3.0 Unported Licence.

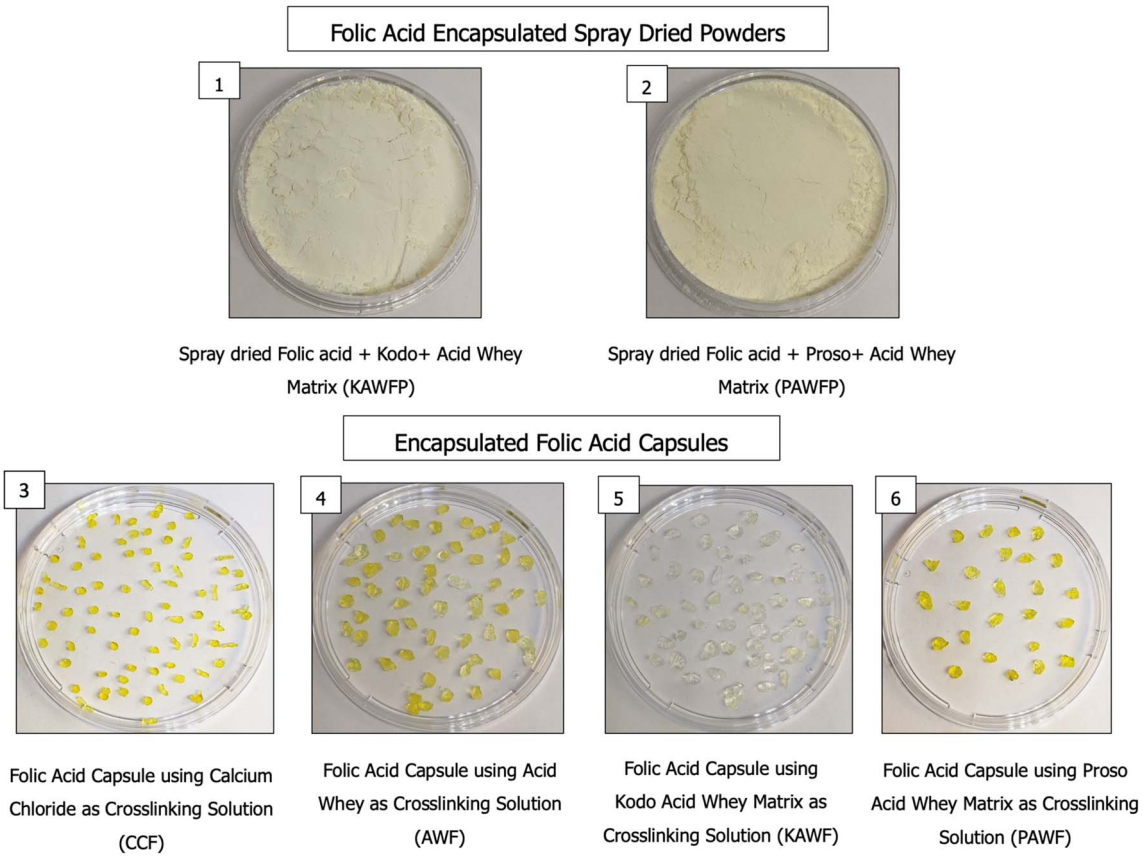

Fig. 3 Folic acid encapsulated powder was developed using kodo millet KAWFP[1] and developed using proso millet PAWFP.[2] Folic acid capsules were developed using different crosslinking solutions such as calcium chloride CCF,[3] acid whey AWF,[4] kodo & acid whey solution KAWF,[5] and proso & acid whey solution PAWF.[6]

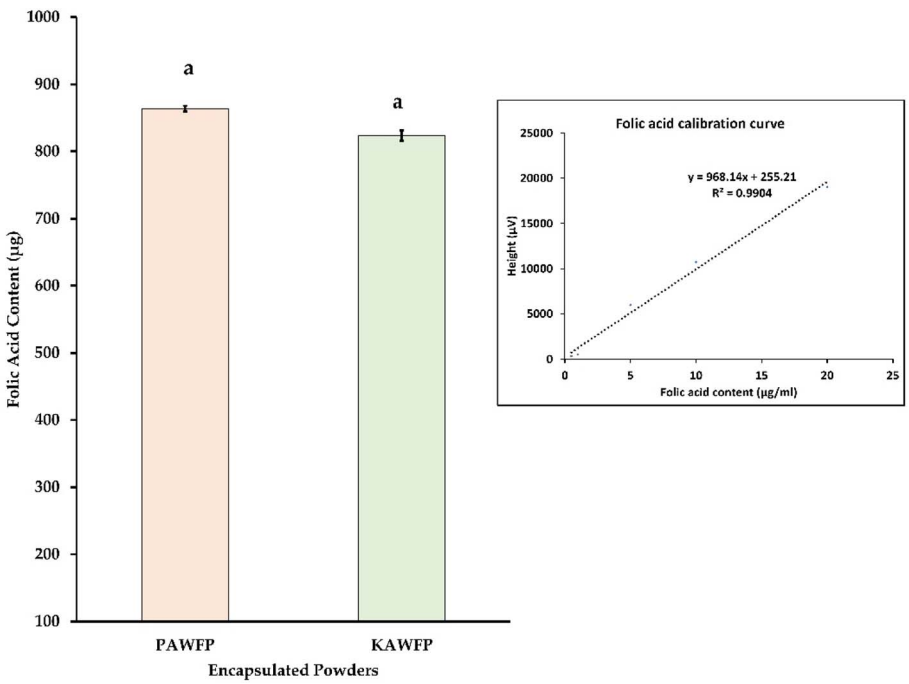

Fig. 4 Folic acid amount (µg) encapsulated by spray drying 100 mL of matrix consisting of acid whey, millets, and folic acid calculated using the calibration curve. The same letters on the bar graph indicate there was no significant difference ($p > 0.05$) among the samples.

Open Access Article. Published on 21 April 2023. Downloaded on 1/12/2026 11:32:11 PM.
This article is licensed under a Creative Commons Attribution-NonCommercial 3.0 Unported Licence.

body post-ingestion.[28] In comparison, the protein and carbohydrates present in acid whey and millets are much healthier options to be used as an encapsulant or a wall material. The protein present in acid whey include lactoferrin, β-lactoglobulin, α-lactalbumin, immunoglobulins, bovine serum albumin (BSA), lysozymes *etc.* The amino acid profile includes primarily lysine, tryptophan, and leucine. Additionally, lactose is the main (4.18% w/v) sugar present in acid whey.[29] It has been observed that partial replacement of whey protein with lactose can help in limiting the diffusion of apolar substances through the formed wall.[30] Likewise, millets are high-protein (11% in kodo and 17% in proso millet) food with a rich carbohydrate composition of starch, cellulose, free sugar, xylose, fructose, maltose, glucose, sucrose, raffinose, maltotriose, and other oligosaccharides.[31]

Furthermore, an alternate method consisting of extrusion-based encapsulation was also performed with sodium alginate, acid whey, and millets to form folic acid capsules. Alginate is an anionic polymer derived from brown seaweed that has high biocompatibility and low toxicity. The components of the polymeric chain of alginate include β-D-mannuronic acid (M blocks) and α-L-guluronic acid (G blocks) wherein they are linked by glycosidic linkages.[1–4] When the monovalent ion of sodium alginate is exchanged with divalent or trivalent ions, the low viscosity liquid usually changes to a gel-like structure. The overall gel strength depends on the molecular weight, structure, and concentration of the gelling agent. Calcium-dependent gelation is one such technique that is extensively used in Industry. Based on the gelation process, there can be the formation of egg box model like structure, 3/1 or 2/1 helical conformation.[32] Various studies have reported that calcium ions lead to dimerization of the polymer chain by forming junction zones that also have further lateral interactions wherein weak inter-dimer associations occur because of electrostatic interactions.[33] Acid whey contains minerals as one of its main constituents wherein a considerable amount of calcium, potassium, sodium, zinc *etc.*, can be found.[34] It has been reported that the concentration of calcium in acid whey and zinc is three times greater than that of sweet whey.[35] Similarly, millets are also rich in minerals such as calcium, copper, iron, potassium, magnesium, *etc.*[36] Consequently, when folic acid mixed with alginate was dropped into the acid whey solution, capsules were formed as shown in Fig. 3. For this product, a significant difference was observed in terms of folic acid in different crosslinking solutions, but no significant difference observed for folic acid encapsulated in capsules as shown in Fig. 5.

The encapsulation efficiency varied from 4.09–6.77% for the capsules and 11.33–47.06% for the cross-linking solution. Fig. 5 shows the folic acid amount obtained from 100 mL of the final product that consisting of capsules as well as the crosslinking solution. In a similar study, Azevedo *et al.*,[37] used alginate/chitosan nanoparticles to encapsulate vitamin B2 wherein an efficiency of about 56% was observed. The study suggested there is a direct relation between encapsulation efficiency and particle size.

3.2 Color analysis

Color is one of the most important sensory properties of a food product as it is an indicator of food quality and flavor. It helps the industry to be consistent and uniform with the food product. Folic acid is available as multivitamins and individual supplements in form of yellow uncoated tablets. Being photosensitive, it is easily degraded and hence, it is important to analyze the color of the form product. When combined with acid whey and millets, the powder had a high lightness value (L)

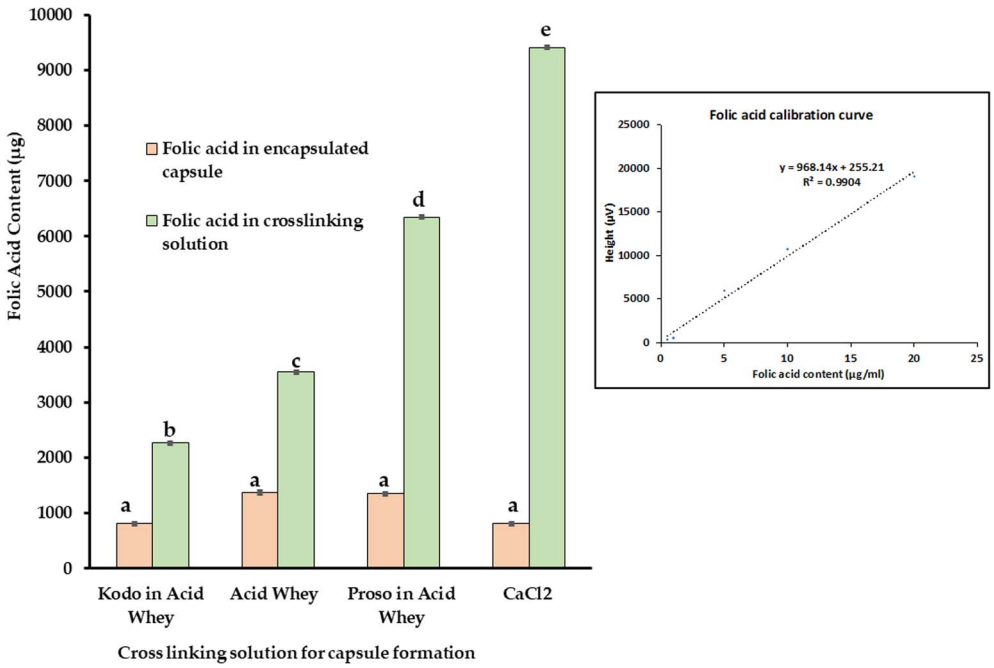

Fig. 5 Folic acid content is obtained in capsules and cross-linking solutions when 20 mL alginate folic acid solution is dispensed in 100 mL crosslinking solution. Different letters on the bar graph indicate a significant difference ($p < 0.05$) among the samples.

 © 2023 The Author(s). Published by the Royal Society of Chemistry

Open Access Article. Published on 21 April 2023. Downloaded on 1/12/2026 11:32:11 PM.
This article is licensed under a Creative Commons Attribution-NonCommercial 3.0 Unported Licence.

Table 1 Color (L, a & b values), moisture content and water activity values for the folic acid encapsulated products[a]

Samples	Color (L)	Color (a)	Color (b)	Hue angle	Chroma	Whiteness index	Moisture content	Water activity
KAWFP	97.56 ± 0.0^{a}	-2.93 ± 0.00^{d}	12.03 ± 0.02^{e}	103.68 ± 0.03^{a}	12.38 ± 0.02^{e}	87.38 ± 0.02^{a}	4.60 ± 0.98^{e}	0.30 ± 0.00^{b}
PAWFP	96.81 ± 0.05^{b}	-3.14 ± 0.01^{e}	15.06 ± 0.02^{d}	101.77 ± 0.00^{c}	15.38 ± 0.00^{d}	84.29 ± 0.00^{b}	3.91 ± 0.15^{f}	0.30 ± 0.00^{b}
CCF	81.79 ± 0.04^{f}	-0.84 ± 0.01^{b}	22.36 ± 0.01^{c}	92.14 ± 0.01^{e}	22.38 ± 0.01^{c}	71.15 ± 0.03^{d}	96.42 ± 0.49^{a}	0.95 ± 0.00^{a}
AWF	82.50 ± 0.02^{e}	-2.95 ± 0.02^{d}	29.94 ± 0.14^{a}	95.62 ± 0.02^{d}	30.08 ± 0.14^{a}	65.19 ± 0.19^{f}	94.27 ± 0.54^{b}	0.95 ± 0.00^{a}
KAWF	84.60 ± 0.02^{c}	-2.37 ± 0.00^{c}	10.17 ± 0.01^{f}	103.13 ± 0.03^{b}	10.44 ± 0.01^{f}	81.39 ± 0.02^{c}	93.83 ± 0.24^{c}	0.95 ± 0.00^{a}
PAWF	83.96 ± 0.10^{d}	0.07 ± 0.03^{a}	28.23 ± 0.13^{b}	89.85 ± 0.06^{f}	28.23 ± 0.13^{b}	67.53 ± 0.07^{e}	92.07 ± 0.27^{d}	0.95 ± 0.00^{a}

[a] Different superscripts indicate significantly different values of mean ($p < 0.05$) in the same column.

of 97.56 and 96.81 for KAWFP and PAWFP respectively as shown in Table 1. For the gel samples, the lightness (L) value was highest for kodo based sample (KAWF). All the samples except PAWFA had a negative "a" value indicating green color. The positive "b" value of all the samples indicated the yellow color of the powder. The hue of a color is the first color that is perceived indicating the dominant wavelength wherein 0° or 360° describes red color, 90° yellow, 180° indicates green and 270° stands for blue color. The hue value validated that the color of the samples was observed as yellow and green color. Similarly, chroma describes the purity of a particular observed in a product. A high chroma value indicates that the color observed is in its purest form.[38] Acid whey had the highest chroma value as compared to other products. Similarly, the whitening index, describes the rating of a white or a near-white surface in terms of distance away from a nominal white coordinate wherein the L value is equivalent to 100 and a, b values are zero.[39] Hence, a high WI_D indicates a high value for whiteness and *vice versa*. The highest whiteness value was observed for the KAWFP powder sample.

3.3 Moisture content and water activity

Moisture content indicates the amount of water present in a product that can influence its properties. Water activity explains the unbound water in the product that is available for the growth of microorganisms. If the water activity is more than

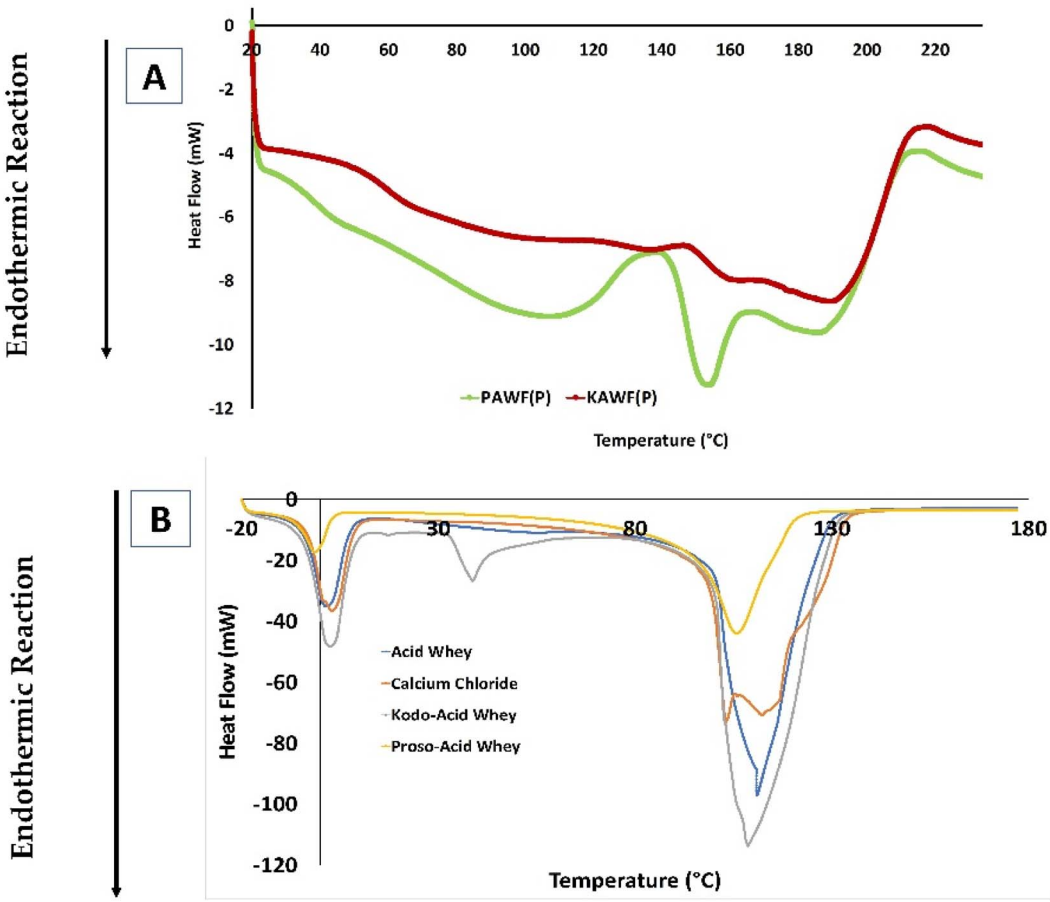

Fig. 6 Thermal degradation of powder samples (A) and capsule samples (B) indicating the peak melting temperature for the samples.

Open Access Article. Published on 21 April 2023. Downloaded on 1/12/2026 11:32:11 PM.
This article is licensed under a Creative Commons Attribution-NonCommercial 3.0 Unported Licence.

Table 2 Peak degradation & glass transition temperature were obtained for the developed encapsulated products

S. no	Samples	Peak degradation temp. (°C)	Glass transition temperature (°C)
1	KAWFP	148.63 ± 1.93	152.19 ± 1.36
2	PAWFP	148.83 ± 6.13	143.18 ± 5.76
3	CCF	107.68 ± 6.49	96.60 ± 3.67
4	AWF	109.17 ± 2.61	83.795 ± 5.73
5	KAWF	111.04 ± 3.40	100.02 ± 1.51
6	PAWF	107.95 ± 2.95	97.3 ± 0.169

0.9, there are more chances for the growth of pathogenic bacteria.[40] The moisture content and water activity for the capsules were observed to be high as shown in Table 1. However, for the powder sample, the moisture content and water activity were low indicating low microbial growth susceptibility. Moisture also affects the flow of the powder by interacting either with the surface or penetrating the bulk of the solid. It leads to physicochemical changes depending on the extent of the hydrophilic properties of the product. Typically, the target moisture content for the food powder industry ranges between 0.3–4%. Also, if the water activity is around 0.3, the food product is microbiologically safe.

3.4 Thermal analysis

The glass transition temperature is an indication that at what temperature the material changes from a rigid to a flexible state. Initially, at room temperature, the particles exhibit an amorphous state wherein there is a random arrangement of the molecule and as the temperature increases, the structure of the molecule changes to become a bit more flexible. In food processing, a lower glass transition temperature indicates that the food is soft and elastic and a higher describes the hardness and brittle properties of food. Similarly, melting temperature, T_m, describes the peak temperature wherein complete melting of organic compounds occurs. Fig. 6 illustrates the thermogram obtained for the samples and Table 2 describes the corresponding glass transition temperature. The glass transition temperature of spray dried powder was higher as compared to the encapsulated capsules. It was observed that there was no difference in-between the encapsulated powders ($p > 0.05$). Table 2 summarizes all the glass transition and peak degradation temperatures for all the samples. However, since all the developed products are made with ingredients having a complex composition of macro and micronutrients, it is difficult to point at the exact glass transition temperature.

Water acts as a plasticizer in powder products as it modifies the glass transition temperature. Consequently, the moisture content of a product is a key factor that affects the glass transition temperature wherein as the moisture content increases, there is the decrease in the glass transition temperature.[41] It also helps in understanding the shelf stability of a powder as it explains about wettability and solubility of the powder.

3.5 Particle size analysis

The particle size observed for the encapsulated powders was found to be statistically similar ($p > 0.05$). The distribution curve as shown in Fig. 7 illustrates the intensity distribution of different sizes. The scattering intensity of a particle is proportional to the square of the molecular weight. Table 3 summarizes the characterization of encapsulated powder particles in terms of polydispersity index (PDI), D10, D50, D90, and zeta potential values. The PDI indicates the heterogeneity of the sample obtained by taking the ratio of the average molecular weight of particles and the number of particles. A higher PDI (PDI > 1) indicates that the molecular weight has been distributed over a broader range as observed in the case of PAWFP. The distribution can also be characterized by D10, D50 and D90 values on the distribution curve wherein these values are defined by the point where 10%, 50%, and 90% of the particles fall below the distribution curve respectively as shown in Fig. 7. Likewise, zeta potential helped in estimating the physical stability of the particles. It is the potential difference between the dispersion medium and the layer of dispersed medium attached to the particle that is dispersed. If the zeta potential is high, the particles are more stable as compared to low zeta

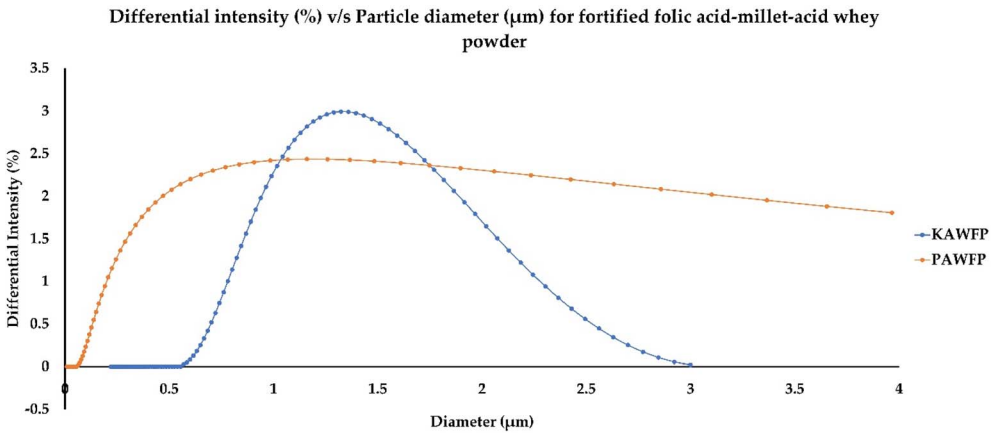

Fig. 7 Intensity distribution curve for the spray dried powders KAWFP and PAWFP corresponding to the cumulant diameter of 1.20 ± 0.13 and 1.13 ± 0.02 μm respectively.

 © 2023 The Author(s). Published by the Royal Society of Chemistry

Open Access Article. Published on 21 April 2023. Downloaded on 1/12/2026 11:32:11 PM.
This article is licensed under a Creative Commons Attribution-NonCommercial 3.0 Unported Licence.

Table 3 Particle size characterization of the encapsulated powders KAWFP & PAWFP[a]

Sample	Polydispersity index	D10 (μm)	D50 (μm)	D90 (μm)	Zeta potential
KAWFP	0.80 ± 0.17^{a}	0.80 ± 0.08^{a}	1.22 ± 0.13^{a}	1.86 ± 0.2^{a}	-9.96 ± 1.30^{a}
PAWFP	1.09 ± 0.62^{a}	0.21 ± 0.08^{a}	1.10 ± 0.20^{a}	6.69 ± 0.27^{b}	-8.44 ± 0.49^{a}

[a] Different superscripts indicate significantly different values of mean ($p < 0.05$) in the same column.

potential wherein the particles tend to aggregate due to the present van der Waal forces. If the magnitude of zeta potential (mV) lies between 0 to 5, it corresponds to matrix that has rapid coagulation, 10 to 30 describes incipient instability, 30 to 40 stands for moderate, 40 to 60 for good and more than 61 describes excellent stability.[42] The zeta potential obtained for both the powders was approximately in the range of incipient instability.

The size and sphericity of the encapsulated capsules are affected by the flow rate, alginate concentration, size of the needle, and crosslinking solutions.[43] The average diameter was found to be significantly different ($p < 0.05$) wherein capsules by acid whey crosslinking, AWF (0.180 ± 0.01 cm) was observed to be the largest followed by KAWF (0.154 ± 0.01 cm), PAWF (0.145 ± 0.02 cm) and CCF (0.135 ± 0.01 cm) respectively. In terms of sphericity, PAWF (0.882 ± 0.12) was found to have the highest sphericity as compared to CCF (0.755 ± 0.10), AWF (0.768 ± 0.14), and, KAWF (0.753 ± 0.13).

3.6 Surface morphology and elemental analysis

The surface morphology of the encapsulated powder samples showed the formation of some wrinkled, spherical particles of different sizes as shown in Fig. 8. The heterogeneity in different sizes of the formed powder particles can be attributed to different drying histories of the particles that occurs during the spray drying process.[44] The smaller particles appeared to adhere to larger particles because of the hygroscopicity of the particles that tends to bring particles in closer proximity and cause

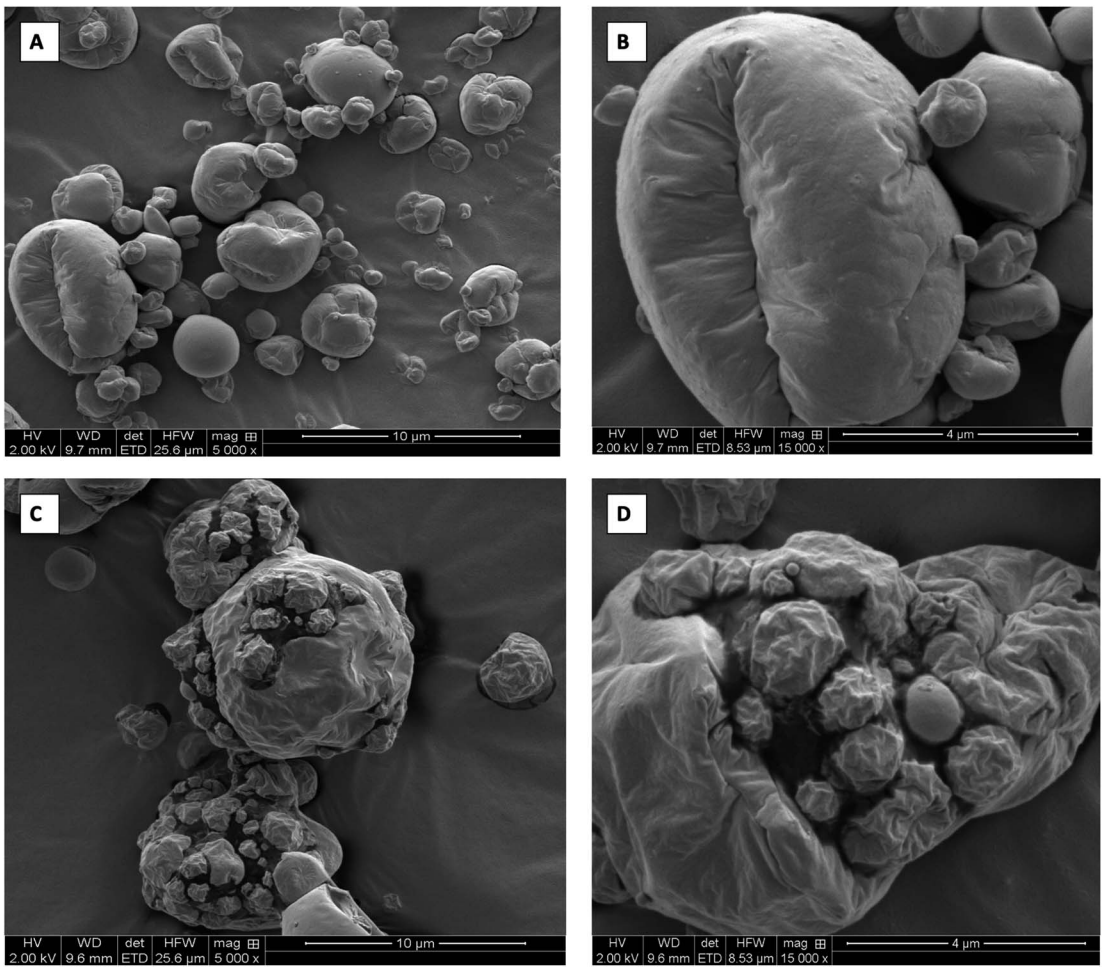

Fig. 8 Scanning electron microscopy of encapsulated folic acid in kodo acid whey matrix (KAWF) at magnification 5000× (A) & 150 00× (B) and proso acid whey matrix (PAWF) at magnification 5000× (C) and 15 000× (D).

Open Access Article. Published on 21 April 2023. Downloaded on 1/12/2026 11:32:11 PM.
This article is licensed under a Creative Commons Attribution-NonCommercial 3.0 Unported Licence.

coalescence. The morphology of the particles also depends on the processing parameters such as inlet temperature, feed rate, aspiration rate, the viscosity of the feed, nozzle type, *etc.* Studies have found that by lowering the inlet temperature and outlet humidity, the wrinkling effect can be reduced on the formed particles which subsequently give higher flowability.[45] The Fig. 9 shows the SEM-EDS analysis of PAWF samples. The images show the presence of minerals such as calcium, potassium, phosphorous, nitrogen, and magnesium that are identified when the characteristic x-rays are generated from material when an electron beam strikes the sample. These x-rays have discrete energies, and the relative intensities of the mapped elements can be compared through the formed spectra that correlate the concentration of that element.[46] The existence of these minerals can be attributed to the millet-acid whey matrix that acts as the cross-linking agent for the formation of these capsules suggesting that they can be potentially used as a source of these micronutrients.

3.7 Stability of folic acid capsules

3.7.1 pH. The pH analysis was conducted at different temperatures and light/dark conditions. Since folates are sensitive to heat, oxygen, and UV light, they tend to change into inactive products under extreme conditions. Hence, to analyze the stability of the food product, it is important to observe how the product performs under different conditions in regard to pH.

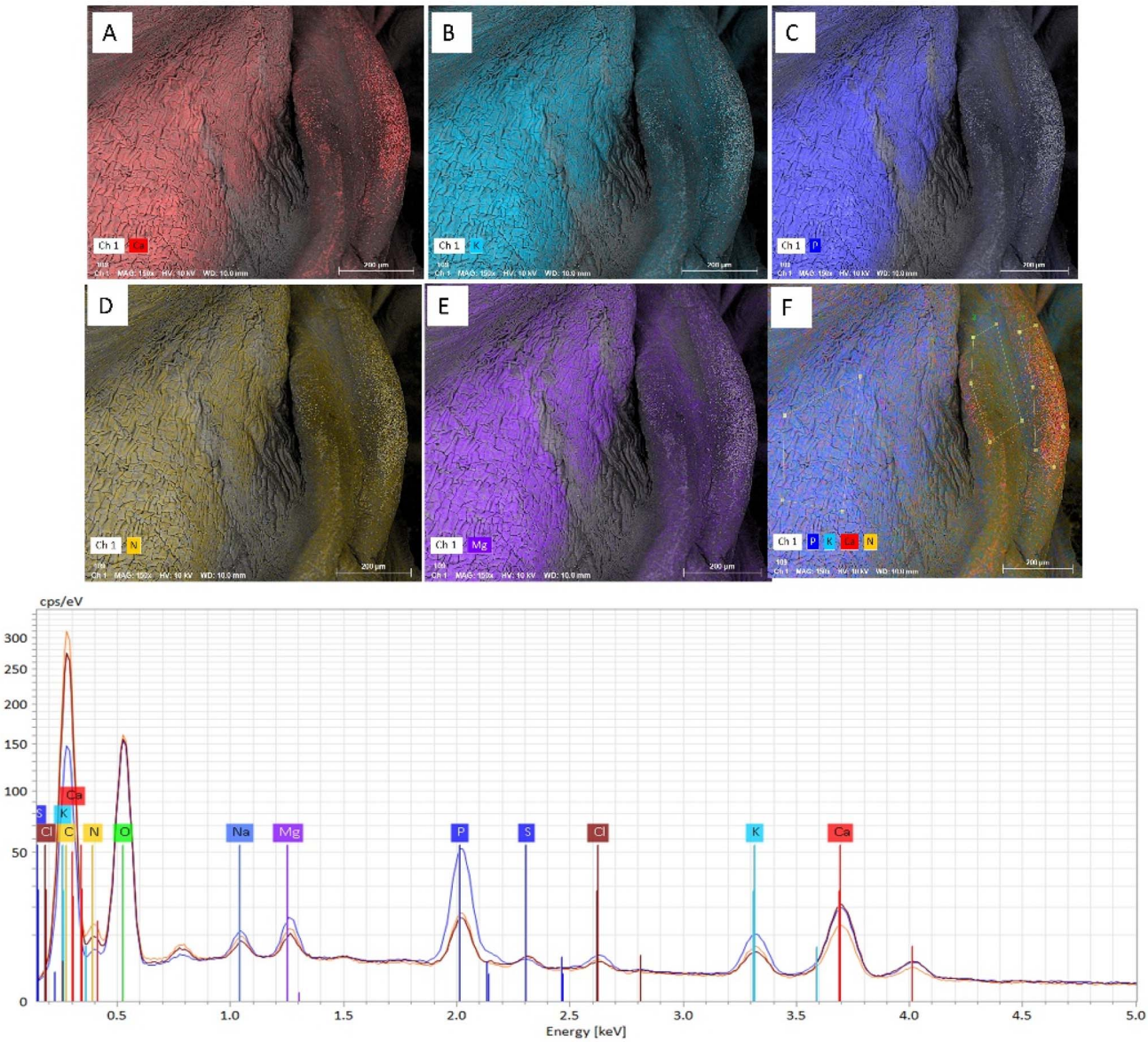

Fig. 9 Elemental analysis of PAWF capsules using electron dispersive X-ray spectroscopy for identification of calcium (A), potassium (B), phosphorous (C), nitrogen (D) and magnesium (E). Part (F) shows the overlap of elements phosphorous, potassium, calcium and nitrogen on the capsule.

 © 2023 The Author(s). Published by the Royal Society of Chemistry

Open Access Article. Published on 21 April 2023. Downloaded on 1/12/2026 11:32:11 PM.
This article is licensed under a Creative Commons Attribution-NonCommercial 3.0 Unported Licence.

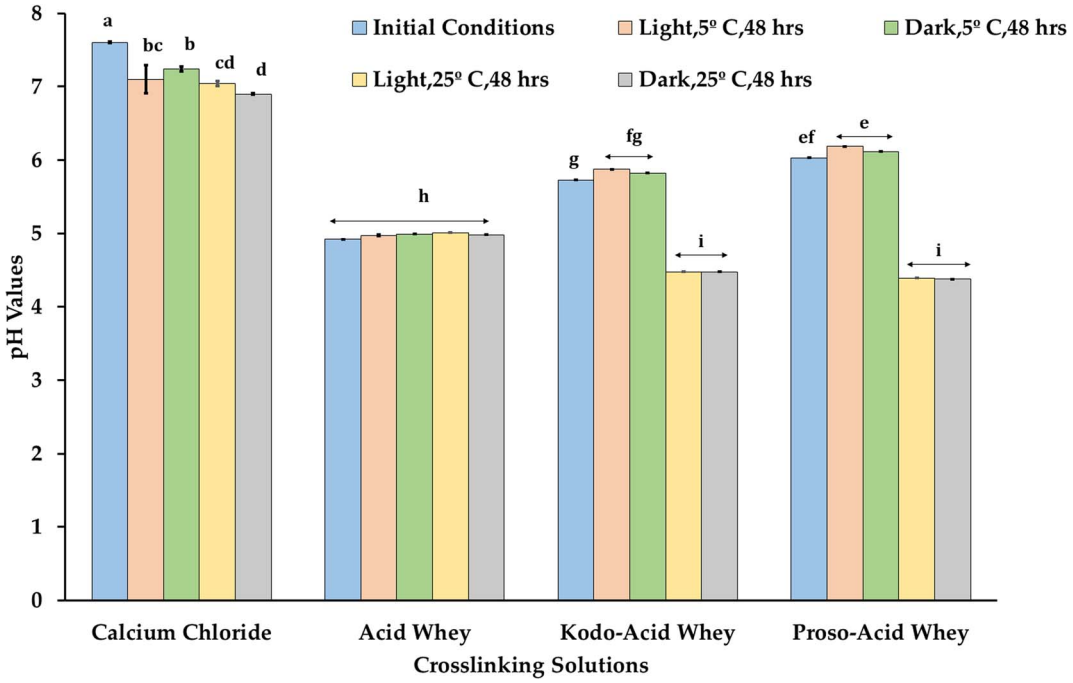

Fig. 10 pH change of the encapsulated capsules kept in different crosslinking solutions for 48 hours under different temperatures (5 and 25 °C) and light conditions (light & dark). Different letters on the bar graph indicate significant differences among the samples ($p < 0.05$).

The highest initial pH was observed for calcium chloride (CCF) followed by proso-acid whey (PAWF), kodo acid whey (KAWF) and finally acid whey (AWF) as shown in Fig. 10. Acid whey cross-linking solution and capsules were observed to have no pH change after 48 hours indicating stability. Light conditions did not significantly impact the pH change, but the temperature did influence crosslinking solution including calcium chloride, kodo acid whey and proso acid whey. Various studies support that acid, alkali, and UV conditions affect the degradation of folic acid wherein acidic conditions degrade more than the alkali conditions. It has also been reported that storage of folic acid should be stored in a container that has minimum penetration of UV light.[47,48]

3.7.2 Mechanical stability. The mechanical stability of capsules explains their ability to withstand the shear forces and changes in the environment. In a similar experiment conducted by Bhujbal *et al.*,[49] factors that influence the mechanical stability of alginate-based microencapsulated cells were analyzed and it was observed that gelling time, gelling, and storage solution were the main factors impacting the firmness of the capsule.

According to the observed hardness value, as shown in Fig. 11, the capsules made from calcium chloride (CCF) cross-linking solution exerted the maximum force followed by proso-acid whey-based capsule (PAWF). The acid whey based (AWF) and kodo acid whey based (KAWF) capsules exerted similar force. The steadiness of an alginate-based capsule depends on the alginate type, concentration, and the type of cation involved in gelling. Proso has a rich mineral profile with 0.23 g/100 g calcium, 0.4 g/100 g phosphorous, 2.24 g/100 g potassium, 0.26 g/100 g magnesium, 25 mg kg^{-1} iron, 16.3 mg kg^{-1} copper and 18.5 mg kg^{-1} zinc.[50] These minerals can act as a source of cations (Ca^{2+}, Mg^{2+}, Zn^{2+} *etc.*) that induce gelling. In addition, these cations can also affect the ionic radii, thickness, tensile strength, and moisture content of the resultant alginate film.[51]

3.8 Functional properties of spray dried powder

Density of a food powder is an important parameter for the determination of handling and storage conditions. It also affects the flowability and appearance of the powder. Density can be categorized into absolute, bulk, and tap density. Absolute density does not account for the open pores and voids present in the powder while doing the volume measurement. However, the bulk density considers the pore spaces in the volume measurement as the material is made to conform to the irregular contour of the container. Hence, using the values of absolute density and bulk density, the porosity of a material can be determined. Likewise, tap density also accounts for interparticle voids but tends to have optimum packing of particles. For the spray dried powders, a significantly higher absolute density was observed indicating that the material was porous as shown in the Table 4.

According to Carr's Index and Hausner ratio, both the powders were in the range of excellent flowability (Hausner ratio 1–1.11 & Carr Index < 10). Flowability can also be determined using the angle of repose wherein if a powder gives a higher value, the powder is then considered to be stickier and has lower flowability. Conversely, if the angle of repose is low, the powder is considered to be free-flowing. For both the powder samples a lower angle of repose was observed as shown in the table validating the flowability of the powder. There was no significant difference observed in the hygroscopicity of both the powders as shown in Table 4. Various factors impact the angle

Open Access Article. Published on 21 April 2023. Downloaded on 1/12/2026 11:32:11 PM.
This article is licensed under a Creative Commons Attribution-NonCommercial 3.0 Unported Licence.

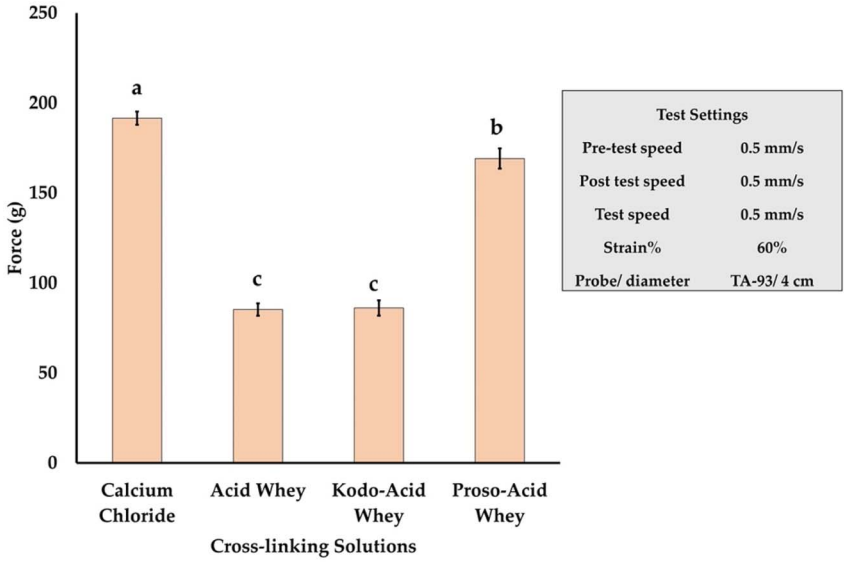

Fig. 11 Hardness value of encapsulated capsules made from different crosslinking solutions. Different letters on the bar graph indicate significant difference among the samples ($p < 0.05$).

Table 4 Functional characterization of spray dried encapsulated powder including density, flowability and reconstitution properties[a]

Functional property	KAWFP	PAWFP
True density (kg m^{-3})	2370 ± 16.3^{a}	1583.33 ± 30.9^{b}
Tap density (kg m^{-3})	492.06 ± 11.2^{a}	366.30 ± 12.9^{b}
Bulk density (kg m^{-3})	468 ± 10.2^{a}	337.60 ± 14.4^{b}
Porosity	0.80 ± 0.00^{a}	0.70 ± 0.01^{b}
Carr index	4.60 ± 0.10^{b}	7.83 ± 1.32^{a}
Hausner ratio	1.05 ± 0.00^{a}	1.09 ± 0.02^{a}
Angle of repose (°)	23.03 ± 0.91^{b}	25.60 ± 0.69^{a}
Hygroscopicity	0.26 ± 0.04^{a}	0.27 ± 0.02^{a}
Brix (%)	11.80 ± 0.0^{a}	10.35 ± 0.05^{b}
Water solubility (%)	95.00 ± 2.9^{a}	92.00 ± 2.2^{a}
Dispersibility (%)	97.17 ± 1.3^{a}	98.59 ± 1.75^{a}
Viscosity (mPa s^{-1})	1.18 ± 0.02^{a}	1.22 ± 0.04^{a}

[a] Different superscripts indicate significantly different values of the mean ($p < 0.05$) in the same row.

of repose and hygroscopicity of a spray dried powder specifically the inlet temperature of the spray dryer that further determines the moisture content of the powder.[52] If the inlet temperature is too high, the lower amount of moisture content results in to the powder that further increases the tendency of the powder to gain moisture present in the air.[53]

A powdered drink mix should not take time for dissolving and agglomerate when coming in contact with water. Henceforth, in terms of reconstitution properties, it was observed that both the powders were highly soluble and dispersible in water. Reconstitution properties determines the quality of a food product and depends on the composition of the product, particle size, charge, density, on processing conditions. For example, the presence of hydrophilic components such as sucrose increases the solubility and dissolution rate.[54] Similarly, when the treatment temperature is too high, the denaturation of proteins decreases the solubility.[55] Considering folic acid is sparingly soluble under neutral pH water conditions, mixing in millets and acid whey helped in its viability as a commercial product that can be used as the folic acid source.

Similarly, rheological analysis helps in validating the processing parameters and consequently in their improvement. It factors in when the processing requires steps such as mixing, dispensing, pumping, cleaning, *etc.* wherein it can determine the volumetric flow rates, pump selection, heat transfer coefficients, *etc.*[56] Viscosity explains a fluid's resistance to flow that impacts the flow and texture of a product.[57] It has also been found that it has a strong association with satiety. The viscosity of the reconstituted samples was found to be similar to water (1 mPa s^{-1} at 20 °C) and fruit juices (1.53–300 mPa s^{-1}).[58] Hence, according to the obtained data, Newtonian flow behavior was observed wherein shear stress (σ) was observed to be in direct proportion to strain rate (s^{-1}). Furthermore, there is a linear relationship between viscosity and refractive index.[59] The Brix percentage corresponds to the sugar content in the product that must be regulated for maintaining consistency. The refractive index changes with concentration, temperature, and different pressure conditions.[60] In between the powders KAWFP and PAWFP, there was a significant difference ($p < 0.5$) obtained in terms of the refractive index wherein kodo based formulation had the higher value. The dissimilarity can be attributed to the difference in the sugar profile in the millets and the extent of absorption of millets in the acid whey.

3.9 *In vitro* digestibility of samples

The *in vitro* digestion analysis helps in the determination of the amount of folic acid that will be absorbed in blood after it goes through the digestion process. The digestion process mainly consists of the mouth, stomach, and intestine wherein α-amylase, trypsin, pepsin and lipase are the major digestive

 © 2023 The Author(s). Published by the Royal Society of Chemistry

Open Access Article. Published on 21 April 2023. Downloaded on 1/12/2026 11:32:11 PM.
This article is licensed under a Creative Commons Attribution-NonCommercial 3.0 Unported Licence.

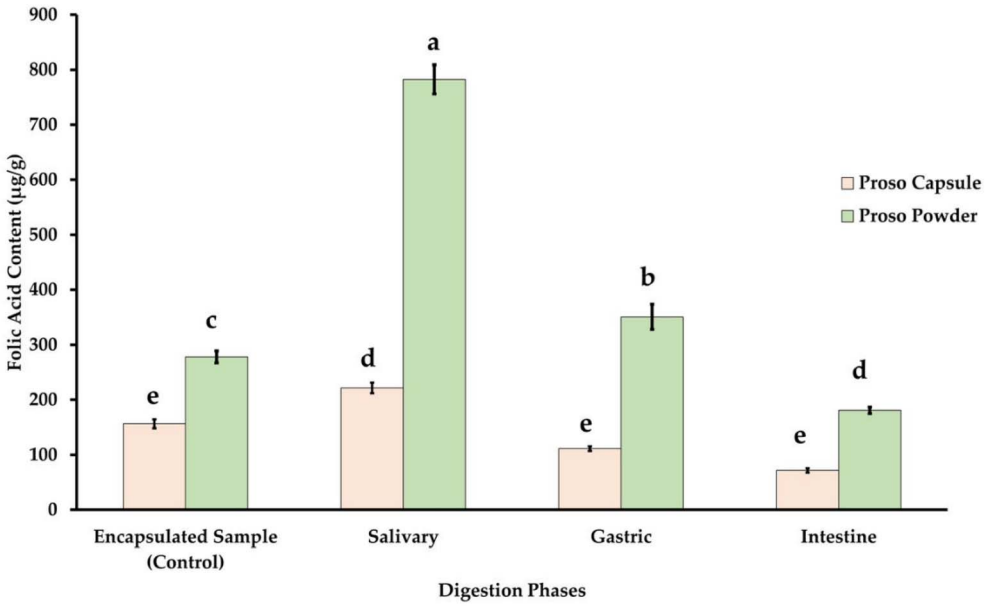

Fig. 12 Folic acid bioaccessibility during digestion phases from proso based encapsulated Powder (PAWFP) and capsule (PAWF) sample. Different letters on the bar graph indicate significant difference among the samples ($p < 0.05$).

enzymes acting on the folic acid. Proso based encapsulated capsules (PAWF) and encapsulated powder were used for analyzing the *in vitro* digestion. Pure proso millet contains a significant amount of vitamins such as niacin, B-complex vitamin, and folic acid. The folic acid content corresponds to 85 mg/100.[61] The powder samples had a higher bioaccessibility % as compared to the capsule, wherein 45.86% was observed for PAWF and 64.99% was observed for PAWFP. It was observed that in both cases, the salivary phase had maximum release followed by the gastric and intestinal phase. The folic acid release from the powder sample was found to be significantly higher as compared to the capsules ($p < 0.05$) as shown in Fig. 12.

Bioaccessibility describes the release of the ingested nutrient from the food matrix that is available for absorption and is dependent on the digestion phases. For natural food-based folates, factors such as stability before ingestion, during digestion, and the presence of other compounds that might hinder the stability of the vitamin affect the absorption. The absorption occurs when it is converted into monoglutamate by the enzyme pteroylglutamate hydrolase. The presence of organic acids can lead to inhibition of this enzyme. Similarly, folate binding protein can also affect the bioaccessibility of the vitamin based on the pH conditions wherein there is lower binding affinity at pH 5–7.4.[62]

Various studies have confirmed that folic acid is highly stability after *in vitro* digestion. For example, Neves *et al.*,[63] investigated the thermal and *in vitro* stability of folic acid in bread, the results indicated that 100% folic acid is free for absorption in the small intestine. Shi *et al.*,[64] suggested that folic acid affects the activity of the digestive enzyme α-amylase, pepsin, and trypsin by forming multi non-covalent bonds. It was observed that there is a formation of a complex that consists of folic acid and the enzyme that inhibits the activity of the enzyme wherein α-amylase activity is affected the most and trypsin activity is affected the least.

4 Conclusion

With the prevalence of folate deficiency specifically among women because of insufficient dietary intake, it is important to develop food products that can act as a source. Fortified food as compared to supplements can provide a large variety of macro-micronutrients fulfilling the daily calorie need as well. The products developed in the study were able to encapsulate the daily required amount of folic acid as suggested by the National Institute of Health (NIH) Office of Dietary Supplements. However, the encapsulation efficiency for the development of the process was found to be low. For improvement in encapsulation efficiency, while upscaling the spray drying process, drying aids could be utilized. Adding millets to acid whey led to a high yield percentage of the powder. According to Carr Index and Hausner ratio values, the obtained powder was free flowing in nature. The high-water solubility and high dispersibility percentage indicated improvement in the limited aqueous solubility of folic acid that can help in commercial viability. The encapsulated capsules were found to be shelf-stable at refrigerated temperature. Proso-acid whey crosslinking solution was able to form the capsule with the highest hardness value. The *in vitro* digestibility model also validated that powder mix and alginate capsules were an efficient delivery system for folic acid.

Data availability

The data supporting the results of this study are available from the corresponding author, Kiruba Krishnaswamy.

Open Access Article. Published on 21 April 2023. Downloaded on 1/12/2026 11:32:11 PM.
This article is licensed under a Creative Commons Attribution-NonCommercial 3.0 Unported Licence.

Author contributions

Sargun Malik: methodology, investigation, writing-original draft, visualization, software. Mohamed B. Bayati: methodology, investigation, writing-review & editing, software. Chung-Ho Lin: methodology, resources, writing-review & editing, supervision. Kiruba Krishnaswamy: conceptualization, methodology, resources, visualization, software, writing-review & editing, supervision, project administration, funding acquisition.

Conflicts of interest

There are no conflicts to declare.

Acknowledgements

We are thankful for the University of Missouri Startup funds to the Food Engineering and Sustainable Technologies (FEAST) program. Biorender was used to make graphical abstract.

References

1 WHO, *Anaemia in women and children*, 2021, available from: **https://www.who.int/data/maternal-newborn-child-adolescent-ageing/advisory-groups/gama/gama-related-resources/gho**.

2 B. A. Campbell, Megaloblastic Anemia in Pregnancy, *Clin. Obstet. Gynecol.*, 1995, **38**(3), 455. Available from: **https://journals.lww.com/clinicalobgyn/Fulltext/1995/09000/Megaloblastic_Anemia_in_Pregnancy.5.aspx**.

3 CDC, *Folic Acid. Centers for Disease Control and Prevention*, 2021, available from: **https://www.cdc.gov/ncbddd/folicacid/about.html**.

4 NIH, Office of Dietary Supplements, *Folate – Health Professional Fact Sheet*, 2020, available from: **https://ods.od.nih.gov/factsheets/Folate-HealthProfessional/**.

5 M. V. de M. Ribeiro, I. da S. Melo, F. das C. Lopes and G. C. Moita, Development and validation of a method for the determination of folic acid in different pharmaceutical formulations using derivative spectrophotometry, *Braz. J. Pharm. Sci.*, 2016, **52**(4), 741–750. Available from: **https://www.scielo.br/scielo.php?script=sci_arttext&pid=S1984-82502016000400741&lng=en&tlng=en**.

6 M. R. I. Shishir, L. Xie, C. Sun, X. Zheng and W. Chen, Advances in micro and nano-encapsulation of bioactive compounds using biopolymer and lipid-based transporters, *Trends Food Sci. Technol.*, 2018, **78**, 34–60. Available from: **https://linkinghub.elsevier.com/retrieve/pii/S092422441730777X**.

7 R. Pérez-Masiá, R. López-Nicolás, M. J. Periago, G. Ros, J. M. Lagaron and A. López-Rubio, Encapsulation of folic acid in food hydrocolloids through nanospray drying and electrospraying for nutraceutical applications, *Food Chem.*, 2015, **168**, 124–133. Available from: **https://linkinghub.elsevier.com/retrieve/pii/S030881461401084X**.

8 K. S. Ravichandran and K. Krishnaswamy, Sustainable food processing of selected North American native berries to support agroforestry, *Crit. Rev. Food Sci. Nutr.*, 2021, 1–26. Available from: **https://www.tandfonline.com/doi/full/10.1080/10408398.2021.1999901**.

9 C. Anandharamakrishnan and S. P. Ishwarya, *Spray Drying Techniques for Food Ingredient Encapsulation: Anandharamakrishnan/Spray Drying Techniques for Food Ingredient Encapsulation*, John Wiley & Sons, Ltd, Chichester, UK, 2015, available from: **https://doi.wiley.com/10.1002/9781118863985**.

10 D. Li, Z. Wei and C. Xue, Alginate-based delivery systems for food bioactive ingredients: An overview of recent advances and future trends, *Compr. Rev. Food Sci. Food Saf.*, 2021, **20**(6), 5345–5369. Available from: **https://onlinelibrary.wiley.com/doi/10.1111/1541-4337.12840**.

11 K. Y. Lee and D. J. Mooney, Alginate: Properties and biomedical applications, *Prog. Polym. Sci.*, 2012, **37**(1), 106–126. Available from: **https://linkinghub.elsevier.com/retrieve/pii/S0079670011000918**.

12 R. A. Neff, R. Kanter and S. Vandevijvere, Reducing Food Loss And Waste While Improving The Public's Health, *Health Affairs*, 2015, **34**(11), 1821–1829. Available from: **https://www.healthaffairs.org/doi/10.1377/hlthaff.2015.0647**.

13 A. Brandelli, D. J. Daroit and A. P. F. Corrêa, Whey as a source of peptides with remarkable biological activities, *Food Res. Int.*, 2015, **73**, 149–161. Available from: **https://linkinghub.elsevier.com/retrieve/pii/S0963996915000319**.

14 E. Singh and A. Sarita, Nutraceutical and food processing properties of millets: a review, *Austin Journal of Nutrition and Food Sciences*, 2016, **4**, 1077.

15 D. M. W. D. Divisekera, J. K. R. R. Samarasekera, C. Hettiarachchi, J. Gooneratne, M. I. Choudhary, S. Gopalakrishnan, *et al.*, Lactic acid bacteria isolated from fermented flour of finger millet, its probiotic attributes and bioactive properties, *Ann. Microbiol.*, 2019, **69**(2), 79–92, DOI: **10.1007/s13213-018-1399-y**.

16 S. Malik, K. Krishnaswamy and A. Mustapha, Physical properties of complementary food powder obtained from upcycling of Greek yogurt acid whey with kodo and proso millets, *J. Food Process Eng.*, 2021, **44**(11). Available from: **https://onlinelibrary.wiley.com/doi/10.1111/jfpe.13878**.

17 K. Skryplonek, I. Dmytrów and A. Mituniewicz-Małek, Probiotic fermented beverages based on acid whey, *J. Dairy Sci.*, 2019, **102**(9), 7773–7780. Available from: **https://linkinghub.elsevier.com/retrieve/pii/S0022030219305995**.

18 D. Rajmohan and D. Bellmer, Characterization of Spirulina-Alginate Beads Formed Using Ionic Gelation, *Int. J. Food Sci.*, 2019, 7101279. Available from: **https://pubmed.ncbi.nlm.nih.gov/31058183**.

19 P. Micha, Physical Properties of Food Powders, *Food Engineering Westport*, AVI Publishing, 1983, pp. 293–324.

20 J. Fitzpatrick, Powder properties in food production systems, in *Handbook of Food Powders*, Elsevier, 2013, pp. 285–308. Available from: **https://linkinghub.elsevier.com/retrieve/pii/B9780857095138500121**.

21 E. Juarez-Enriquez, G. I. Olivas, E. Ortega-Rivas, P. B. Zamudio-Flores, S. Perez-Vega and D. R. Sepulveda,

 © 2023 The Author(s). Published by the Royal Society of Chemistry

Open Access Article. Published on 21 April 2023. Downloaded on 1/12/2026 11:32:11 PM.
This article is licensed under a Creative Commons Attribution-NonCommercial 3.0 Unported Licence.

Water activity, not moisture content, explains the influence of water on powder flowability, *LWT*, 2019, **100**, 35–39. Available from: https://linkinghub.elsevier.com/retrieve/pii/S0023643818308892.

22 N. Jinapong, M. Suphantharika and P. Jamnong, Production of instant soymilk powders by ultrafiltration, spray drying and fluidized bed agglomeration, *J. Food Eng.*, 2008, **84**(2), 194–205. Available from: https://linkinghub.elsevier.com/retrieve/pii/S0260877407002853.

23 M. Minekus, M. Alminger, P. Alvito, S. Ballance, T. Bohn, C. Bourlieu, *et al.*, A standardised static *in vitro* digestion method suitable for food – an international consensus, *Food Funct.*, 2014, **5**(6), 1113–1124. Available from: https://xlink.rsc.org/?DOI=C3FO60702J.

24 I. I. Muhamad, N. D. Hassan, S. N. H. Mamat, N. M. Nawi, W. A. Rashid and N. A. Tan, Extraction Technologies and Solvents of Phytocompounds From Plant Materials : Physicochemical Characterization and Identification of Ingredients and Bioactive Compounds From Plant Extract Using Various Instrumentations, in *Ingredients Extraction by Physicochemical Methods in Food*, Elsevier, 2017, pp. 523–560, available from: https://linkinghub.elsevier.com/retrieve/pii/B9780128115213000144.

25 B. Fox, G. Bellini and L. Pellegrini, Drying, in *Fermentation and Biochemical Engineering Handbook*, Elsevier, 2014, pp. 283–305, available from: https://linkinghub.elsevier.com/retrieve/pii/B9781455725533000143.

26 S. Malik, K. Krishnaswamy and A. Mustapha, Development and functional characterization of complementary food using kodo and proso millet with acid whey from Greek yogurt processing, *J. Food Process. Preserv.*, 2021, **46**(9), available from: https://onlinelibrary.wiley.com/doi/10.1111/jfpp.16051.

27 X. S. Liang, F. Q. Zhao and L. X. Hao, Research on Stability of Synthetic Folic Acid, *Adv. Mater. Res.*, 2013, **781–784**, 1215–1218. Available from: https://www.scientific.net/AMR.781-784.1215.

28 D. L. Hofman, V. J. van Buul and F. J. P. H. Brouns, Nutrition, Health, and Regulatory Aspects of Digestible Maltodextrins, *Crit. Rev. Food Sci. Nutr.*, 2016, **56**(12), 2091–2100. Available from: https://www.tandfonline.com/doi/full/10.1080/10408398.2014.940415.

29 D. Rocha-Mendoza, E. Kosmerl, A. Krentz, L. Zhang, S. Badiger, G. Miyagusuku-Cruzado, *et al.*, Invited review: Acid whey trends and health benefits, *J. Dairy Sci.*, 2021, **104**(2), 1262–1275. Available from: https://linkinghub.elsevier.com/retrieve/pii/S0022030220310559.

30 A. Gharsallaoui, G. Roudaut, O. Chambin, A. Voilley and R. Saurel, Applications of spray-drying in microencapsulation of food ingredients: an overview, *Food Res. Int.*, 2007, **40**(9), 1107–1121. Available from: https://linkinghub.elsevier.com/retrieve/pii/S0963996907001238.

31 D. B. Wankhede, A. Shehnaj and M. R. Raghavendra Rao, Carbohydrate composition of finger millet (Eleusine coracana) and foxtail millet (Setaria italica), *Plant Foods Hum. Nutr.*, 1979, **28**(4), 293–303. Available from: https://link.springer.com/10.1007/BF01095511.

32 H. Wang, D. Li, C. Wan, Y. Luo, Q. Yang, X. Gao, *et al.*, Improving the Functionality of Proso Millet Protein and Its Potential as a Functional Food Ingredient by Applying Nitrogen Fertiliser, *Foods*, 2021, **10**(6), 1332. Available from: https://www.mdpi.com/2304-8158/10/6/1332.

33 H. Wang, Y. Wan, W. Wang, W. Li and J. Zhu, Effect of calcium ions on the III steps of self-assembly of SA investigated with atomic force microscopy, *Int. J. Food Prop.*, 2018, **21**(1), 1995–2006. Available from: https://www.tandfonline.com/doi/full/10.1080/10942912.2018.1494200.

34 J. Chandrapala, M. C. Duke, S. R. Gray, B. Zisu, M. Weeks, M. Palmer, *et al.*, Properties of acid whey as a function of pH and temperature, *J. Dairy Sci.*, 2015, **98**(7), 4352–4363. Available from: https://linkinghub.elsevier.com/retrieve/pii/S0022030215003094.

35 N. P. Wong, D. E. LaCroix and F. E. McDonough, Minerals in Whey and Whey Fractions, *J. Dairy Sci.*, 1978, **61**(12), 1700–1703. Available from: https://linkinghub.elsevier.com/retrieve/pii/S0022030278837904.

36 A. Vinoth and R. Ravindhran, Biofortification in Millets: A Sustainable Approach for Nutritional Security, *Front. Plant Sci.*, 2017, **8**. Available from: https://journal.frontiersin.org/article/10.3389/fpls.2017.00029/full.

37 M. A. Azevedo, A. I. Bourbon, A. A. Vicente and M. A. Cerqueira, Alginate/chitosan nanoparticles for encapsulation and controlled release of vitamin B2, *Int. J. Biol. Macromol.*, 2014, **71**, 141–146. Available from: https://linkinghub.elsevier.com/retrieve/pii/S0141813014003328.

38 F. G. Cooper, *The Munsell Book of Color 1929: Hue, Value & Chroma. Munsell Color System; Color Matching from Munsell Color Company*, 2016, available from: https://munsell.com/color-blog/munsell-book-of-color-1929-hue-value-chroma/.

39 M. del M. Pérez, R. Ghinea, M. J. Rivas, A. Yebra, A. M. Ionescu, R. D. Paravina, *et al.*, Development of a customized whiteness index for dentistry based on CIELAB color space, *Dent. Mater.*, 2016, **32**(3), 461–467. Available from: https://linkinghub.elsevier.com/retrieve/pii/S0109564115005114.

40 N. H. Mermelstein, *Measuring Moisture Content & Water Activity - IFT.org*, 2009, available from: https://www.ift.org/news-and-publications/food-technology-magazine/issues/2009/november/columns/laboratory.

41 Y. Wang and T. Truong, Glass Transition and Crystallization in Foods, in *Non-Equilibrium States and Glass Transitions in Foods*, Elsevier, 2017, pp. 153–172, available from: https://linkinghub.elsevier.com/retrieve/pii/B9780081003091000079.

42 A. Kumar and C. K. Dixit, Methods for characterization of nanoparticles, in *Advances in Nanomedicine for the Delivery of Therapeutic Nucleic Acids*, Elsevier, 2017, pp. 43–58, available from: https://linkinghub.elsevier.com/retrieve/pii/B9780081005576000031.

43 A. Partovinia and E. Vatankhah, Experimental investigation into size and sphericity of alginate micro-beads produced by electrospraying technique: Operational condition optimization, *Carbohydr. Polym.*, 2019, **209**, 389–399.

Open Access Article. Published on 21 April 2023. Downloaded on 1/12/2026 11:32:11 PM.
This article is licensed under a Creative Commons Attribution-NonCommercial 3.0 Unported Licence.

Available from: https://linkinghub.elsevier.com/retrieve/pii/S0144861719300190.

44 D. E. Walton, The morphology of spray-dried particles a qualitative view, *Drying Technol.*, 2000, **18**(9), 1943–1986. Available from: https://www.tandfonline.com/doi/abs/10.1080/07373930008917822.

45 E. M. Both, R. M. Boom and M. A. I. Schutyser, Particle morphology and powder properties during spray drying of maltodextrin and whey protein mixtures, *Powder Technol.*, 2020, **363**, 519–524. Available from: https://linkinghub.elsevier.com/retrieve/pii/S0032591020300012.

46 J. Heath and N. Taylor, Energy Dispersive Spectroscopy, *The Atrium, Southern Gate*, John Wiley & Sons, Ltd, Chichester, West Sussex, PO19 8SQ, 2015.

47 G. Pamunuwa, N. Anjalee, D. Kukulewa, C. Edirisinghe, F. Shakoor and D. N. Karunaratne, Tailoring of release properties of folic acid encapsulated nanoparticles via changing alginate and pectin composition in the matrix, *Carbohydr. Polym. Technol. Appl.*, 2020, **1**, 100008. Available from: https://linkinghub.elsevier.com/retrieve/pii/S2666893920300086.

48 S. Yakubu and J. Muazu, Effects of variables on degradation of folic acid, *J. Pharm. Sci.*, 2010, **4**, 55–58.

49 S. V. Bhujbal, G. A. Paredes-Juarez, S. P. Niclou and P. de Vos, Factors influencing the mechanical stability of alginate beads applicable for immunoisolation of mammalian cells, *J. Mech. Behav. Biomed. Mater.*, 2014, **37**, 196–208. Available from: https://linkinghub.elsevier.com/retrieve/pii/S1751616114001532.

50 J. Kalinová, Nutritionally Important Components of Proso Millet (*Panicum miliaceum* L.), *Food Global Science Book*, 2006, vol. 10, pp. 91–100.

51 B. A. Harper, S. Barbut, L. T. Lim and M. F. Marcone, Effect of Various Gelling Cations on the Physical Properties of "Wet" Alginate Films: Effect of various gelling cations on, *J. Food Sci.*, 2014, **79**(4), E562–E567. Available from: https://onlinelibrary.wiley.com/doi/10.1111/1750-3841.12376.

52 D. W. Dadi, S. A. Emire, A. D. Hagos and J. B. Eun, Effects of spray drying process parameters on the physical properties and digestibility of the microencapsulated product from *Moringa stenopetala* leaves extract, *Cogent Food Agric.*, 2019, **5**(1), 1690316. Available from: https://www.tandfonline.com/doi/full/10.1080/23311932.2019.1690316.

53 A. Manickavasagan, K. Thangavel, S. R. S. Dev, D. S. A. Delfiya, E. Nambi, V. Orsat, *et al.*, Physicochemical Characteristics of Date Powder Produced in a Pilot-Scale Spray Dryer, *Drying Technol.*, 2015, **33**(9), 1114–1123. Available from: https://www.tandfonline.com/doi/full/10.1080/07373937.2015.1014045.

54 D. Seth, H. N. Mishra and S. C. Deka, Functional and reconstitution properties of spray-dried sweetened yogurt powder as influenced by processing conditions, *International Journal of Food Properties*, 2017, **20**(7), 1603–1611. Available from: https://www.tandfonline.com/doi/full/10.1080/10942912.2016.1214965.

55 M. B. Perez-gago and J. M. Krochta, Denaturation Time and Temperature Effects on Solubility, Tensile Properties, and Oxygen Permeability of Whey Protein Edible Films, *J. Food Sci.*, 2001, **66**(5), 705–710. Available from: https://onlinelibrary.wiley.com/doi/10.1111/j.1365-2621.2001.tb04625.x.

56 C. I. Nindo, J. Tang, J. R. Powers and P. Singh, Viscosity of blueberry and raspberry juices for processing applications, *J. Food Eng.*, 2005, **69**(3), 343–350. Available from: https://linkinghub.elsevier.com/retrieve/pii/S0260877404003826.

57 K. McCrickerd, L. Chambers, J. M. Brunstrom and M. R. Yeomans, Subtle changes in the flavour and texture of a drink enhance expectations of satiety, *Flavour.*, 2012, **1**(1), 20. Available from: https://flavourjournal.biomedcentral.com/articles/10.1186/2044-7248-1-20.

58 P. Rai, G. C. Majumdar, S. DasGupta and S. De, Prediction of the viscosity of clarified fruit juice using artificial neural network: a combined effect of concentration and temperature, *J. Food Eng.*, 2005, **68**(4), 527–533. Available from: https://linkinghub.elsevier.com/retrieve/pii/S0260877404003152.

59 R. T. Lagemann, A Relation between Viscosity and Refractive Index, *J. Am. Chem. Soc.*, 1945, **67**(3), 498–499, DOI: 10.1021/ja01219a509.

60 A. Belay and G. Assefa, Concentration, Wavelength and Temperature Dependent Refractive Index of Sugar Solutions and Methods of Determination Contents of Sugar in Soft Drink Beverages using Laser Lights, *J. Laser Opt. Photonics*, 2018, **5**(2), DOI: 10.4172/2469-410X.1000187.

61 D. K. Santra and D. J. Rose, *Alternative Uses of Proso Millet*, The board of Regents of the University of Nebraska, 2013, vol. 4.

62 P. Etcheverry, M. A. Grusak and L. E. Fleige, Application of in vitro bioaccessibility and bioavailability methods for calcium, carotenoids, folate, iron, magnesium, polyphenols, zinc, and vitamins B6, B12, D, and E, *Front Physio.*, 2012, **3**, 317. Available from: https://journal.frontiersin.org/article/10.3389/fphys.2012.00317/abstract.

63 D. A. Neves, K. B. d. S. Lobato, R. S. Angelica, J. Teixeira Filho, G. P. R. d. Oliveira and H. T. Godoy, Thermal and in vitro digestion stability of folic acid in bread, *J. Food Compos. Anal.*, 2019, **84**, 103311. Available from: https://linkinghub.elsevier.com/retrieve/pii/S0889157519306192.

64 W. Shi, Y. Wang, H. Zhang, Z. Liu and Z. Fei, Probing deep into the binding mechanisms of folic acid with α-amylase, pepsin and trypsin: An experimental and computational study, *Food Chem.*, 2017, **226**, 128–134. Available from: https://linkinghub.elsevier.com/retrieve/pii/S0308814617300547.

 © 2023 The Author(s). Published by the Royal Society of Chemistry